AD-A169 602 INTRINSIC SIO2 FILM STRESS MEASUREMENTS ON THERMALLY OXIDIZED SI(U) NORTH CAROLINA UNIV AT CHAPEL HILL DEPT OF CHEMISTRY E KOBEDA ET AL. 20 JUN 86 TR-7 1/1

UNCLASSIFIED N00014-83-K-0571 F/G 7/4 NL

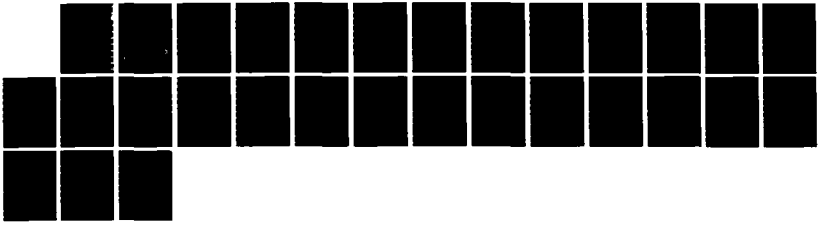

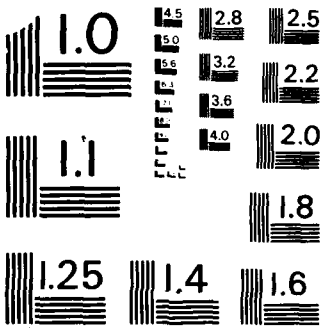

OFFICE OF NAVAL RESEARCH

Contract No. N00014-83-K-0571

Task No. NR 625-843

TECHNICAL REPORT NO. 7

INTRINISIC SiO_2 FILM STRESS MEASUREMENTS ON THERMALLY OXIDIZED Si

by

E. Kobeda and E.A. Irene
Dept. of Chemistry
The University of North Carolina
Chapel Hill, NC 27514

in

J. Vac. Sci. and Technology

SECURITY CLASSIFICATION OF THIS PAGE

ADA 169602

REPORT DOCUMENTATION PAGE

1a REPORT SECURITY CLASSIFICATION Unclassified	1b RESTRICTIVE MARKINGS
2a SECURITY CLASSIFICATION AUTHORITY	3 DISTRIBUTION/AVAILABILITY OF REPORT Approved for public release; distribution unlimited.
2b DECLASSIFICATION/DOWNGRADING SCHEDULE	
4 PERFORMING ORGANIZATION REPORT NUMBER(S) Technical Report #7	5 MONITORING ORGANIZATION REPORT NUMBER(S)
6a NAME OF PERFORMING ORGANIZATION UNC Chemistry Dept.	6b OFFICE SYMBOL (If applicable)
6c ADDRESS (City, State and ZIP Code) 11-3 Venable Hall 045A Chapel Hill, NC 27514	7a NAME OF MONITORING ORGANIZATION Office of Naval Research (Code 413) 7b ADDRESS (City, State and ZIP Code) Chemistry Program 800 N. Quincy Street Arlington, Virginia 22217
8a NAME OF FUNDING/SPONSORING ORGANIZATION Office of Naval Research	8b OFFICE SYMBOL (If applicable)
8c ADDRESS (City, State and ZIP Code) Chemistry Program 800 N. Quincy, Arlington, VA 22217	9 PROCUREMENT INSTRUMENT IDENTIFICATION NUMBER Contract #N00014-83-K-0571 10 SOURCE OF FUNDING NOS

PROGRAM ELEMENT NO	PROJECT NO	TASK NO	WORK UNIT NO
		NR625-843	

11 TITLE (Include Security Classification) INTRINSIC SiO_2 FILM STRESS MEASUREMENTS ON THERMALLY OXIDIZED Si

12 PERSONAL AUTHOR(S)
E. Kobeda and E.A. Irene

13a TYPE OF REPORT	13b TIME COVERED	14 DATE OF REPORT (Yr., Mo., Day)	15 PAGE COUNT
Interim Technical	FROM _____ TO _____	6/20/86	26

16 SUPPLEMENTARY NOTATION
Prepared for publication in J. Vac. Sci. and Technol.

17 COSATI CODES			18 SUBJECT TERMS (Continue on reverse if necessary and identify by block number)
FIELD	GROUP	SUB-GR	Silicon Oxidation Silicon Dioxide Properties Thin Film Growth Models

19 ABSTRACT (Continue on reverse if necessary and identify by block number)

We have investigated the effects of varying Si oxidation conditions on intrinsic film stress for SiO_2 films formed on Si. This study includes stress measurements on four Si orientations: (100), (110), (111), and (311); at oxidation temperatures ranging from 700-1100°C; wet (H_2O) vs. dry (O_2) oxidations for (100) and (111) surfaces; and the effects of post-oxidation annealing on stress. We find an orientation dependence for intrinsic stress which scales in the following manner: (110) > (311) > (100) > (111); a reduction in stress for wet vs. dry studies; and an even larger reduction for post-oxidation anneals. A recently proposed step model seems to account for the differences in stress with Si orientation. A number of Si oxidation models based on intrinsic stress are compared in their ability to describe the observed behavior, and we conclude that within the Deal-Grove oxidation model, the linear rate constant is strongly influenced by stress in the initial regime while stress is also likely to be important for thicker films.

20 DISTRIBUTION/AVAILABILITY OF ABSTRACT	21 ABSTRACT SECURITY CLASSIFICATION
UNCLASSIFIED/UNLIMITED ☒ SAME AS RPT ☒ DTIC USERS ☐	Unclassified

22a NAME OF RESPONSIBLE INDIVIDUAL	22b TELEPHONE NUMBER (Include Area Code)	22c OFFICE SYMBOL
Dr. David L. Nelson	(202) 696-4410	

DD FORM 1473, 83 APR EDITION OF 1 JAN 73 IS OBSOLETE

Intrinsic SiO_2 Film Stress Measurements on Thermally Oxidized Si

by

E. Kobeda and E.A. Irene

Dept. of Chemistry

The University of North Carolina

Chapel Hill, N.C. 27514

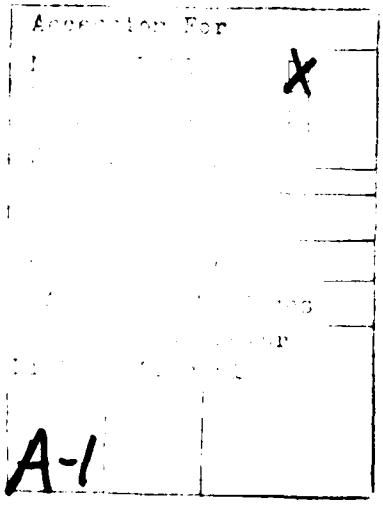

Abstract

We have investigated the effects of varying Si oxidation conditions on intrinsic film stress for SiO_2 films formed on Si. This study includes stress measurements on four Si orientations: (100), (110), (111), and (311); at oxidation temperatures ranging from 700-1100°C; wet (H_2O) vs. dry (O_2) oxidations for (100) and (111) surfaces; and the effects of post-oxidation annealing on stress. We find an orientation dependence for intrinsic stress which scales in the following manner: (110) > (311) > (100) > (111); a reduction in stress for wet vs. dry studies; and an even larger reduction for post-oxidation anneals. A recently proposed step model seems to account for the differences in stress with Si orientation. A number of Si oxidation models based on intrinsic stress are compared in their ability to describe the observed behavior, and we conclude that within the Deal-Grove oxidation model, the linear rate constant is strongly influenced by stress in the initial regime while stress is also likely to be important for thicker films.

Introduction

Recent trends in the microelectronics industry have facilitated the need for smaller and faster MOS devices. For technology to continue to advance, a greater understanding of processing and characterization of microelectronic materials is required. The oxidation of Si to SiO_2 for use as gate dielectrics in MOSFET's is probably the most important process step in the fabrication of integrated circuits. As a consequence of scaling, future VLSI advances require smaller film thickness (<200Å) and lower oxidation temperatures (< 900°C).

The kinetics of the thermal oxidation of Si have been explained using the Deal-Grove linear-parabolic model (1). This model seems to work well for thicker oxides grown at higher oxidation temperatures, where kinetics are oxidant transport limited, but does not account for anomalous kinetic behavior (1-4) observed for the initial oxidation regime. In recent years, several studies have reported the observation of an intrinsic SiO_2 film stress resulting from thermal oxidation of Si at low temperatures (5-8). A number of models have been proposed which consider stress to be influential on either the interface reaction (9,10) or the diffusivity of oxidant species through a strained oxide (11,12,13). The origin of the intrinsic film stress has been attributed to a lack of viscous flow in SiO_2 at lower temperatures (<1000°C) (5,7) arising from an inability to accomodate the volume change in converting Si to SiO_2.

We report new measurements on the orientation dependence of stress for four Si orientations ((100), (110), (111), and (311)) using a previously

described visible light double beam reflection technique (8). An orientation dependence has been reported (1-4) for the thermal oxidation of Si, particularly in the early stages of oxidation. More recently, both theoretical (10) and experimental (14) observations have included the effects of mechanical properties on the $Si-SiO_2$ interface and on the early stages of oxidation. Other studies (11,12,13) also include the effects of interfacial stresses on oxidation kinetics using the transport limitation of oxidant through a stressed film. In this study, we utilize the reported stress data to test both the interface and transport models. Since it was reported that high temperature annealing (15) and H_2O oxidation ambients (1,16) alter the oxidation kinetics, we also report in this study the effects of other varying oxidation conditions on intrinsic film stress, viz. wet vs. dry oxidation, and post-oxidation annealing, and then compare these results with the models. We find that a surface step model (17,18) explains our experimental findings and thus surface steps are a potentially important part of the oxidation phenomena.

Experimental Procedures

Sample preparation.

The measurement of intrinsic SiO_2 film stress was performed on four Si substrate orientations: (100), (110), (111), and (311). A slightly modified RCA cleaning method (19) was used to clean all samples prior to oxidation, which was performed under atmospheric pressure using dry O_2 (less than 5 ppm H_2O and .5 ppm hydrocarbons). For all oxidation experiments performed in this study, the furnace was maintained with a flowing N_2 ambient obtained directly

from a LN_2 source when oxidations were not in progress. A series of temperatures from 700-1100°C was investigated for all orientations and samples were usually oxidized together to minimize slight differences in conditions. The Si wafers used were commercially obtained single crystal Si wafers with the following characteristics: (100), (110), (111)- 2 ohm-cm, p-type, 1-1.5 in. diameter; and (311)- 5 ohm-cm, n-type, 1.25 in. diameter. All four orientations were polished on one side and approximately 8-11 mil thick prior to oxidation. For the accurate measurement of strains for this substrate thickness, approximately 1000Å of SiO_2 was required to obtain sufficient deformation (8). The range of oxide thickness was approximately 1000-10,000 Å for the experiments reported in this study. Once the samples were oxidized under normal conditions the SiO_2 film thickness was measured using ellipsometry with an accuracy of $\pm$ 0.01° for the angular settings of the optical components and the angle of incidence, thus yielding less than 2% error in film thickness. After oxidation and thickness measurements, the oxide was removed from the unpolished back side of the wafer and the strain was measured in a manner previously reported (8) and briefly described below.

The effects of oxidizing Si in a H_2O containing ambient were also investigated. A quartz bubbler was placed in series with a gas feed line to the resistively heated furnace, and dry O_2 was bubbled through to provide the wet oxidation ambient at 1 atm pressure. These oxidations were performed on (100) and (111) oriented Si at oxidation temperatures of 700 and 800°C. It should be noted that this experiment was not an actual steam oxidation, since the quartz bubbler was kept at room temperature. It was estimated that this resulted in an order of magnitude less H_2O compared to a typical steam

oxidation, but we anticipate similar oxidation behavior (16). It has been previously established (20,21) that even traces of H_2O profoundly affect the oxidation rate and many physical properties of the SiO_2 film, but in light of the concentration of H_2O (10^5 ppm) in the ambient used here our results are compared directly with steam oxidations.

Post-oxidation anneals were performed on (100) and (111) samples in N_2 for one hour at 1000°C in order to investigate stress relaxation. The samples were initially dry oxidized at 700 and 800°C in 1 atm O_2, and the wafer deformation (strain) was measured. The samples were remeasured after annealing, and a direct comparison of unannealed vs. annealed samples was thus obtained.

Strain measurements.

We have previously reported the details of the use of a double beam (He-Ne laser) reflection technique to measure Si wafer strain resulting from the oxidation process (8). This is accomplished by measuring the deviation of two parallel laser beams which are reflected from a sample. From these measurements the radius of curvature (R) of a sample can be obtained within about 5% error as determined using calibration standards, and the average total stress can be derived according to Stoney (22):

$$\sigma_f = Et_s^2/6(1-v)t_fR \qquad (1)$$

where E and v are Young's modulus and Poisson's ratio of Si, respectively, and t_s and t_f are the substrate and film thickness in meters, respectively. The values of E/1-v for all four Si orientations and SiO_2 are reported in Table 1. Equation (1) is based on the assumption that the stress distribution is isotropic (26) and that no plastic deformation occurs. Since the measurement

was performed at room temperature, equation (1) yields the total film stress, which is the sum of the thermal expansion and the intrinsic stress components. Thermal expansion stress results from a difference in thermal expansion coefficients, α, for Si and SiO_2 as follows:

$$\sigma_{th}(T) = \int_{T}^{Tox} (E/1-v)(\alpha_{SiO_2} - \alpha_{Si})\, dT \qquad (2)$$

where, T_{ox} and T are the oxidation temperature and the temperature at which the stress is measured (room temperature), respectively (27), and E and v are Young's Modulus and Poisson's ratio of the SiO_2 film. If one assumes that Young's Modulus and the thermal expansion coefficient of the film do not change significantly over the temperature range, then equation (2) can be approximated by

$$\sigma_{th} = \underline{/\backslash\alpha/\backslash}TE/(1-v) \qquad (3)$$

Note that the thermal expansion stress is zero at the oxidation temperature and develops as the sample cools to room temperature. Thus, the thermal expansion stress *cannot affect* oxidation kinetics at T_{ox} but could influence other room temperature properties. For Si-SiO_2 samples, σ_{th} results in compression in the oxide since the thermal expansion coefficient of Si is $2.6 \times 10^{-6}\ ^{o}C^{-1}$ (28), and is approximately five times that for SiO_2, $0.52 \times 10^{-6}\ ^{o}C^{-1}$ (25).

By calculating the thermal stress using equation (3), the intrinsic stress can be determined by the difference between the thermal and total stress (Eq. (1)). Thus, the intrinsic film stress σ_i is:

$$\sigma_i = \sigma_f - \sigma_{th} \qquad (4)$$

where σ_f is the total film stress and σ_{th} the thermal expansion stress as shown in the previous equations. Measurements of σ_i in our laboratory resulted in an average standard deviation of approximately 0.5×10^9 dyn/cm^2,

obtained over all temperatures reported.

Results and Discussion

As pointed out above, a number of relevant oxidation models have been proposed that contain either an explicit or implicit Si orientation dependence and/or characteristic behavior with differing oxidation ambient and/or annealing conditions. In the following sections we discuss some of the published models in view of both our new stress data and other relevant published results. It is instructive to point out here that while we have drawn conclusions from our experimental results on stress, this analysis is based on oxide thicknesses which are for the most part greater than 1000Å. It is conceivable that the observed stresses differ considerably at smaller oxide thickness (early stages of oxidation). A suitable technique for such measurement is not yet available but work on this topic is currently being carried out in our laboratory.

Orientation Effects

Figure 1 shows the intrinsic stress as a function of oxidation temperature for all four orientations studied. We observe that all orientations display an intrinsic compressive SiO_2 film stress that increases with decreasing oxidation temperature. This result agrees both with past stress measurement results (6,7,8) and with the proposed viscous flow model (5,7) which explains the origin of this intrinsic stress as a result of the unsatisfied volume requirement of the oxidation reaction of Si to form a SiO_2 film constrained by

adhesion in the plane of the Si surface. It should be noted that a small numerical error in calculating thermal stress was made in our previous results (8) and in fact no tensile intrinsic stress results in the oxide as suggested by our previous plots demonstrating viscous flow, Figs. 3 and 4, ref. (8). We now recount the essential features of the viscous flow model (7). Figure 2 illustrates that the oxidation caused compressive stress in the x,y plane of Si causes the relaxation of the film into the z direction. Representing SiO_2 as a Maxwell viscoelastic solid, the rate of viscous flow $d\epsilon_z/dt$ for a constant applied stress in the σ_{xy} plane is

$$d\epsilon_z/dt = \sigma_{xy}/\eta_{ox} \qquad (5)$$

where η_{ox} is the oxide viscosity. The rate of viscoelastic relaxation depends on the temperature coefficient of the viscosity, E_η, as shown below:

$$\eta_{ox}(T) = \eta_o \exp(E_\eta/RT) \qquad (6)$$

where η_o is a pre-exponential constant and E_η the energy of activation for viscosity. At higher temperatures, η_{ox} decreases rapidly and the SiO_2 flows freely in the z direction. For low temperature oxidations (< 1000°C), the substantially larger oxide viscosity precludes relaxation during normal oxidation times. The Maxwell model results in the following equation for stress relaxation:

$$\sigma = \sigma_o \exp(-t/\tau) \qquad (7)$$

where σ_o is the maximum oxide stress, t the oxidation time, and τ the characteristic relaxation time (7). In a recent publication (8) we confirmed previous data (5-7) that intrinsic stress increases as a function of decreasing oxidation temperature according to the predictions of this model.

It is apparent that the linear-parabolic, L-P, oxidation model (1) has

neither an explicit Si orientaiton dependence nor any intrinsic stress dependence. This Si oxidation model that considers a steady state in the oxidant flux and the interface reaction results in an integrated rate equation of the form:

$$t-t_o = (L^2-L_o^2)/k_p + (L-L_o)/k_1 \qquad (8)$$

where L and t are the oxide thickness and oxidation time, respectively; L_o and t_o define the initial oxidation regime which does not conform to L-P kinetics; and k_1 and k_p define the linear and parabolic rate constants, respectively. Implicit in k_1 is the number of Si atoms on the particular orientation in question. A modified form of the L-P model has recently been proposed (10). For the present purposes, only the formulation of the revised linear rate constant is germane. The revised k_1 is explicit with respect to the areal density of Si atoms, C_{Si}, intrinsic stress, σ_{xy}, and oxide viscosity, η_{ox} as:

$$k_1 \propto C_{Si}\sigma_{xy}/\eta_{ox} \qquad (9)$$

The orientation dependence is direct through C_{Si} and indirect within σ_{xy}, since the stress is proportional to Young's modulus, E:

$$\sigma = E\epsilon \qquad (10)$$

where ϵ is the strain. This revised model was recently employed to explain a crossover effect observed in the very early stages of oxidation (14) for the major Si orientations ((111), (110), (100)). It was found that the (110) surface exhibited a faster oxidation rate than the (111) in the very early stages of oxidation, with the (111) surface dominating the rate order after a crossover point of characteristic oxide thickness (4,14,24). According to Figure 1 and equation 9 above, we deduce that the (110) should be the fastest oxidizing surface. The (110) not only has the largest areal density of Si

atoms (29) for these three major orientations, but also has the highest measured stress. This finding is somewhat different than was previously reported (14). The previous study was without the benefit of the stress measurements herein reported and relied on theoretical predictions of the orientation behavior of the stress, and therefore it was thought that the orientation dependence of the stress should be ordered according to the orientation dependence of E/1-v. This is so because the oxidation induced strain is constant as a result of the same volume change for all the orientations. This order (24) is as follows:

$$(111) > (110) > (100)$$

and this order should dominate in a stress dominant region. With this in mind, it was previously assumed that this stress dominant regime commenced above the crossover where the (111) Si orientation was found to oxidize the fastest. Now, however, our stress measurements show that the (111) has a small relative stress. Therefore, we now conclude that both areal density and measured oxide stress are important at the outset of the oxidation, and their product scales initially with the oxidation rates according to equation (9). This conclusion is reasonable since the intrinsic stress is tensile in the Si and thus the stretched Si-Si bonds on the surface are likely easier to react. When the oxide becomes sufficiently thick and the diffusion regime commences, the intrinsic compressive oxide stress alters the oxidation order in favor of the (111) since smaller compressive stress in the oxide reduces the diffusivity least for the (111) surface. This latter idea on the effect of stress on diffusivity has been discussed by several authors (11,12,13).

The surface step model proposed by Mott (17) in conjunction with very

recent results of Leroy (18) show how it may be possible to form SiO_2 on Si without the necessity for the buildup of a large intrinsic stress. This Mott model is pictorially illustrated in Figure 3 in which a Si surface with an atomic step is shown. If oxidation takes place predominantly at steps (edge or kink sites), the oxide film advances with a volume expansion laterally as well as normal to the surface. In this manner a large fraction of the stress is relieved as the film grows. While Mott did not discuss an orientation dependence for the substrate, the work of Hahn and Henzler (30) gives evidence for such a relationship. These workers used a LEED technique employing spot broadening measurements to establish that various process parameters such as substrate orientation and oxidation and annealing conditions alter the number of surface steps. In the comparison of (111) and (100) Si orientations under identical treatments, they report approximately a factor of two larger density of edge atoms for (111) samples. Thus, combining this finding with the Mott model we may expect a lower experimental stress than that which is calculated based on the E/1-v value and a constant volume change strain. Therefore we conclude that the revised linear rate constant although accounting for stress and areal Si densities still requires modifications perhaps in accordance with the Mott step model.

Leroy (18) has recently been able to quantitatively account for the orientation dependence of our stress data. He considers the resolution of the biaxial stress in the plane of the variously oxidized Si surfaces to the appropriate slip plane in the Si. He compares this resolved stress, σ-, to the critical shear stress, τ_c, for Si for the orientations. When τ_c is exceeded, defects are produced in the Si which are later oxidized away. The result is

different residual stress. Leroy's calculations require lateral oxidation at steps and is therefore consistent with the Mott step model (17).

The (311) orientation was included for study because it has been reported to have about a 25% greater areal density of Si atoms than the (110) (29) and an intermediate value for E/1-v, although this value is not isotropic in the Si surface (24). In accordance with the revised linear rate constant we might expect a higher initial oxidation rate compared with the (100). However, it has been observed that the (311) surface shows a very similar oxidation rate compared to that for the (100) (24), and therefore a considerably lower rate than the (110) surface. Figure 1 shows comparable stresses for the (311) and (100) planes. While we are not yet certain of the reason for these discrepancies, it is believed that the (311) surface actually has only a slightly greater areal density than the (100) (31) and thus with a similar intrinsic stress should display an oxidation rate similar to the (100) as we observe. This is based on the idea that the (311) plane is vicinal to the (100) and (111) surfaces (24,32). Further work is in progress on this point.

Three recent models (11,12,13) treat the possible effects of stress on the transport of oxidant through an SiO_2 film during oxidation. According to Fargeix et al (12) and Camera Roda et al (13) the conditions that yield the lowest intrinsic stress should also yield the fastest rate, since these authors couple an increased compressive stress with decreased diffusivity. The distribution of stress is also considered to affect the shape of the thickness time oxidation curves. Not readily explained by these stress-diffusion models is our finding that the (110) surface displays both the greatest rate and the largest stress. For larger SiO_2 film thicknesses where the (111) orientation

displays the larger oxidation rate, the stress-diffusion models give the correct order. One study (12) uses this stress-diffusion model to predict the shape of the very initial regime. The model proposed by Doremus (11) has no explicit orientation dependence, but is very similar to the other proposed transport models (12,13) in that it considers D to decrease with increasing compressive stress. Here also the Si orientation dependence in the very initial regime is not explained. Doremus mentions (11) that his model probably does not account for dry O_2 oxidations which exhibit an anomalous initial regime. While with this comment in mind the latter model seems to represent the observations, we show below that intrinsic stress is significantly reduced for H_2O oxidation ambients and thus less effective in altering the oxidation kinetics.

Oxidation Ambient and Annealing

Figures 4 and 5 show that for both the oxidations carried out in an H_2O containing ambient and for post oxidation inert ambient annealing, the resultant intrinsic stress is decreased from the dry oxidation case for both orientations studied. Previous oxidation kinetics studies have shown that H_2O containing O_2 ambients exhibit an increased oxidation rate over the rate due only to the presence of H_2O, a more virulent oxidant than O_2 (14). Since this rate enhancement effect was seen mainly for the parabolic rate constant (16) which is associated with the transport of oxidant (1), this effect was explained by considering the effect of H_2O on transport of the major oxidant, O_2. H_2O is known to react with the Si-O-Si network with the formation of Si-OH groups. The result is a marked decrease in the oxide viscosity (33).

This argument is now further substantiated by the presently reported reduced intrinsic stresses for oxidations performed in the H_2O containing ambients. Furthermore, the present results are in accord with a previous study that showed a reduced relaxation time for the intrinsic stress and refractive index for anneals in a H_2O containing ambient (7). This previous study (7) has also reported intrinsic stress relaxation for an inert ambient anneal, but at a slower rate than for the H_2O containing ambient. This effect of the inert anneal is also confirmed by the present more extensive results. Recent studies (15) show that the oxidation rate is enhanced even after the dry inert ambient anneals. This is consistent with the above mentioned notion that the compressive stress relaxation itself increases the oxidant diffusivity and thus the overall oxidation.

Summary and Conclusions

We have reported the results of a number of studies showing the effects of varying oxidation conditions on intrinsic film stress. It was found that an orientation dependence exists for film stress which may help explain the anomolous behavior observed in the initial regime of Si oxidation kinetics. Other studies included the effects of wet (H_2O) oxidations on stress, and the effects of post-oxidation anneals, where it was found that stress was decreased in both studies, with greater reductions observed for the oxidant grown at 700 °C as compared to 800 °C. We have used both the viscous flow model and an atomic step model to explain the results obtained in these studies. In combination, these two models may lead to a more accurate description of the

kinetic behavior of low temperature thermal oxidations, and consequently increase our understanding of the effects of stress on the linear rate constant.

Acknowledgement

This research was supported in part by the Office of Naval Research (ONR). The authors are particularly indebted to Dr. B. Leroy and E.A. Lewis for their enlightening discussions.

REFERENCES

1. B.E. Deal and A.S. Grove, J. Appl. Phys., 36, 3770 (1965).

2. E.A. Irene and Y.J. van der Meulen, J. Electrochem. Soc.,123, 1380 (1976).

3. H.Z. Massoud, J.D. Plummer, and E.A. Irene, J. Electrochem. Soc.,132, 1745 (1985).

4. H.Z. Massoud, Ph.D. Thesis, Stanford Univ., Stanford, Cal., (1982).

5. E.P. EerNisse, Appl. Phys. Lett., 30, 290 (1977).

6. E.P. EerNisse, Appl. Phys.Lett., 35, 8 (1979).

7. E.A. Irene, E. Tierney, and J. Angillelo, J. Electrochem. Soc., 129, 2594 (1982).

8. E. Kobeda and E.A. Irene, J. Vac. Sci. and Technol. B., 4(3), 720, (1986).

9. W.A. Tiller, J. Electrochem. Soc., 127, 625 (1980).

10. E.A. Irene, J. Appl. Phys., 54, 5416 (1983).

11. R.H. Doremus, Thin Solid Films, 122, 191 (1984)

12. A. Fargeix and G. Ghibaudo, J. Appl. Phys., 56, 589 (1984).

13. G. Camera Roda, F. Santarelli, and G.C. Sarti, J. Electrochem. Soc., 132, 1909 (1985).

14. E.A. Irene, H.Z. Massoud, and E. Tierney, J. Electrochem. Soc., 133, 1253 (1986).

15. J.K. Srivastava and E.A. Irene, J. Electrochem. Soc., 132, 2815 (1985).

16. E.A. Irene and R. Ghez, J. Electrochem. Soc., 124, 1757 (1977).

17. N.F. Mott, Phil. Mag. A, 45 (2), 323 (1981).

18. B. Leroy, "Stresses and Silicon Interstitials During the Oxidation of a Silicon Substrate," presented at the Workshop on Oxidation Mechanisms of the University of Paris 7, May 20-22 1986, Paris, France and to be published in Phil. Mag. 1986/87.

19. W. Kern and D.A. Poutinen, RCA Rev., 31, 187 (1970).

20. W.A. Pliskin, IBM J. of Res. and Develop., 10, 198 (1966).

21. E.A. Irene, J. Electrochem. Soc., 121, 1613 (1974).

22. G.G. Stoney, Proc. Royal Soc. (London) A82, 172 (1909).

23. W.A. Brantley, J. Appl. Phys., 44, 534 (1973).

24. E.A. Lewis, E. Kobeda, and E.A. Irene, Proc. of the Fifth International Symposium on Silicon Materials Science and Technology, The Electrochemical Society, Ed. by H.R. Huff, Boston, Mass., May (1986).

25. Corning Glass Works, Fused Silica, 7940 Data Sheets, Corning, New York, (1978).

26. R.J. Jaccodine and W.A. Schlegel, J. Appl. Phys., 37, 2429 (1966).

27. M. Jarosz, L. Kocsanyi, and J. Giber, Applications of Surface Science, 14, 122 (1982).

28. L. Maissel, J. Appl. Phys., 44, 534 (1973).

29. J.R. Ligenza, J. Phys. Chem., 65, 2011 (1961).

30. P.O. Hahn and M. Henzler, J. Vac. Sci. Technol. A 2(2), 574 (1984).

31. E.A. Lewis, private communication.

32. K. Ueda and M. Inoue, Surf. Sci., 161, L578, (1985).

33. R. Bruckner. J. Non-Crystalline Solids, 5, 123 (1970).

List of Figures

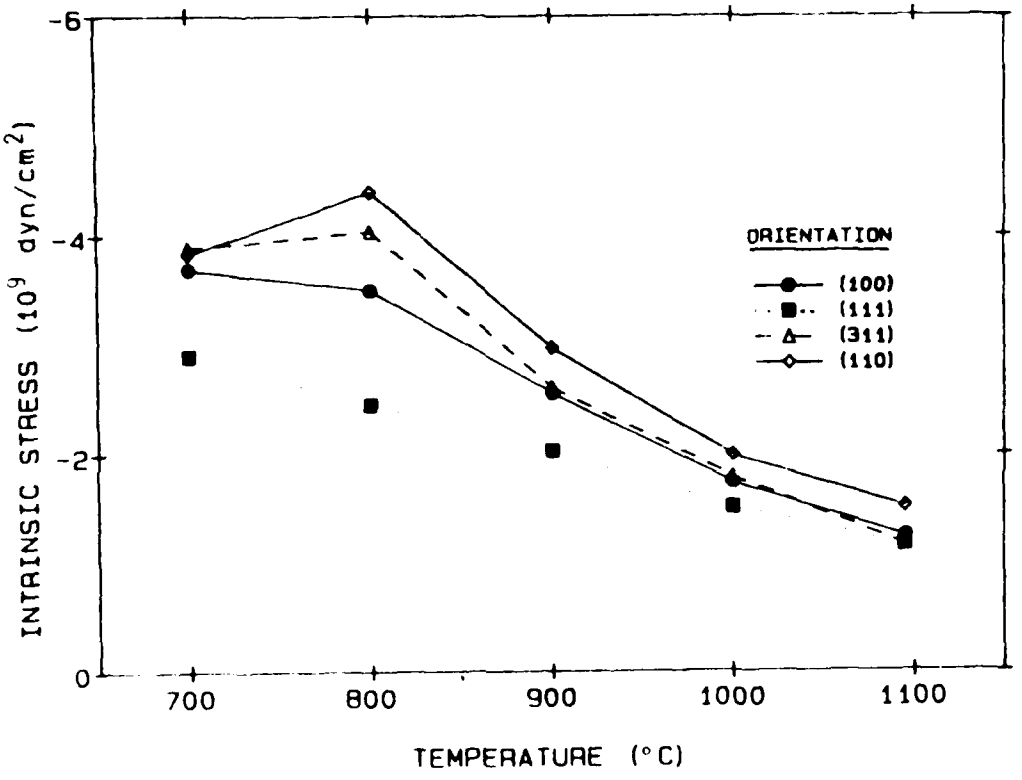
-6
-4
-2
0
INTRINSIC STRESS (10^9 dyn/cm^2)
700
800
900
1000
1100
TEMPERATURE (°C)
ORIENTATION
(100)
(111)
(311)
(110)

Kobeda Fig 1

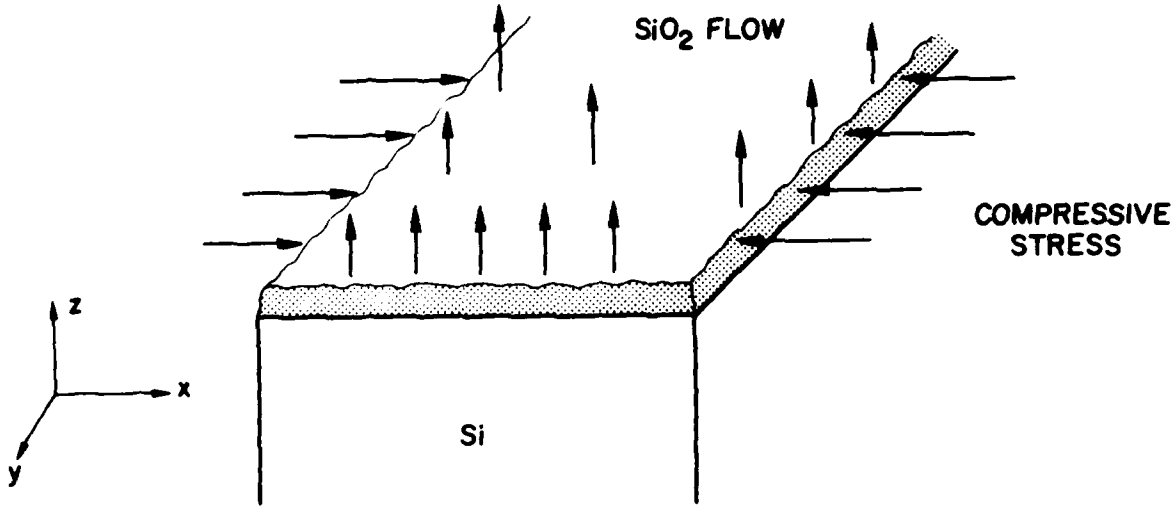

Kobeda Fig 2

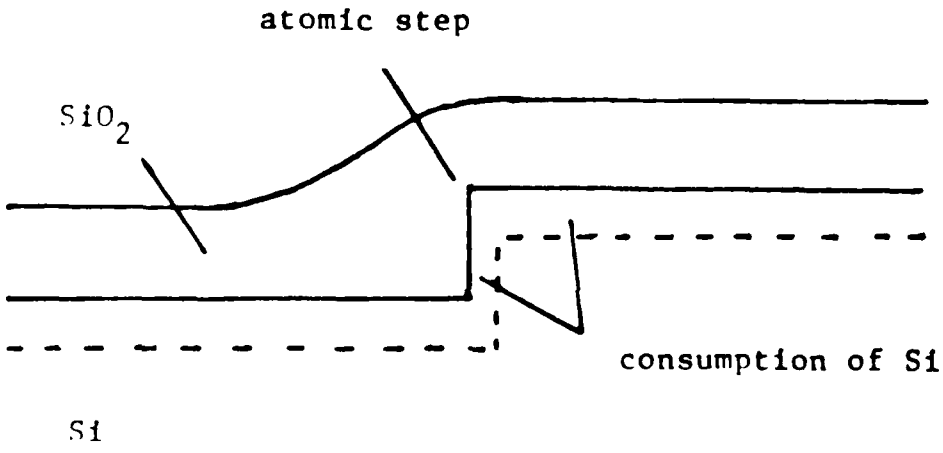

Kobeda Fig 3

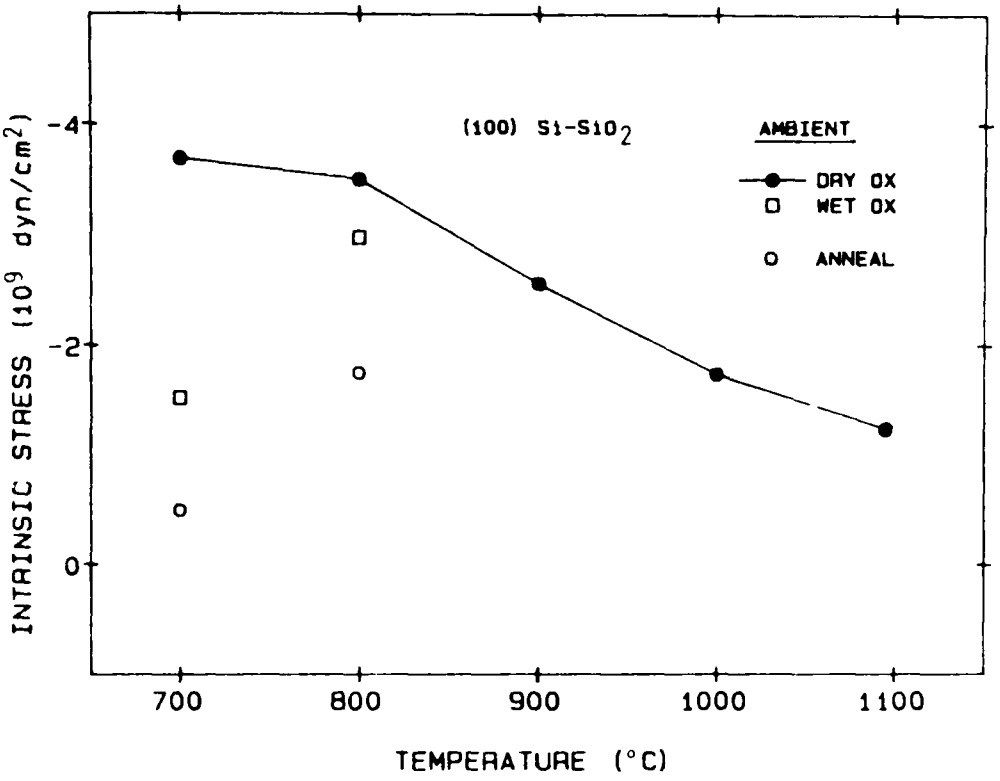
(100) Si-SiO2
AMBIENT
DRY OX
WET OX
ANNEAL
INTRINSIC STRESS (10^9 dyn/cm^2)
-4
-2
0
700
800
900
1000
1100
TEMPERATURE (°C)

Kobeda Fig 4

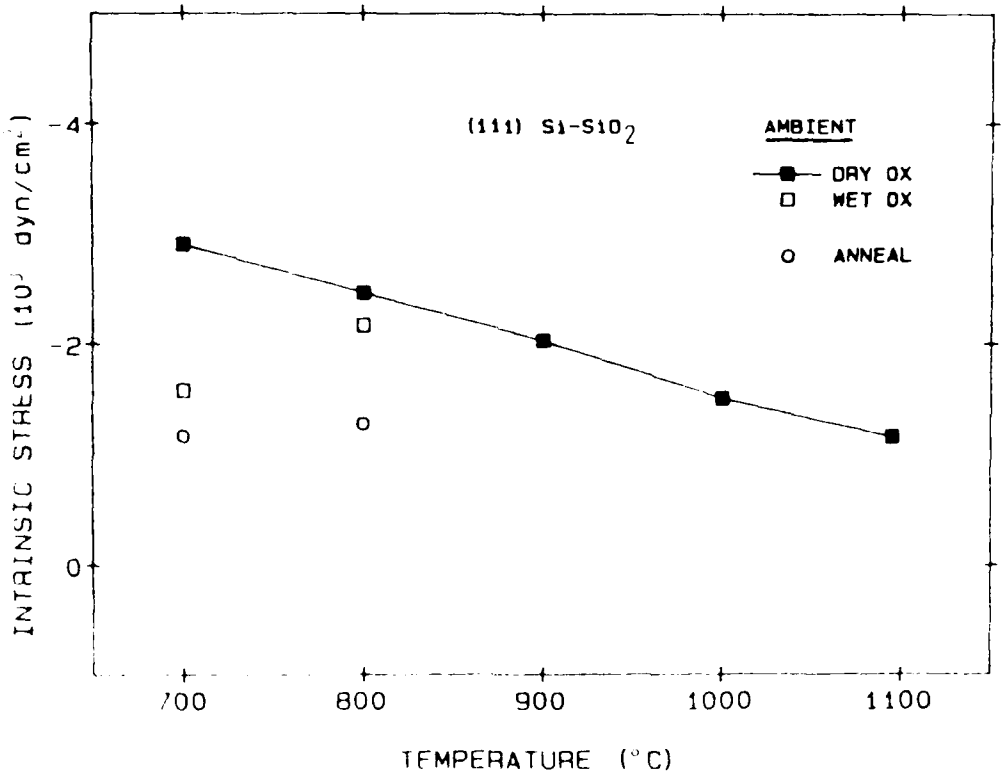
(111) Si-SiO2
AMBIENT
DRY OX
WET OX
ANNEAL
INTRINSIC STRESS (10⁹ dyn/cm²)
-4
-2
0
700
800
900
1000
1100
TEMPERATURE (°C)

Kobeda Fig 5

List of Tables

Si Orientation	E/1-v (10^{12} dyn/cm^2)	Reference
(100)	1.805	23
(110)	2.187	24
(111)	2.290	23
(311)	2.007	24
SiO_2	0.88	25

Table 1. Young's modulus to Poisson's ratio for determination of film stress for Si-SiO_2.

END

DTIC

8-86